RESEARCH ARTICLE

Life Characterization of PEEK and Nanofilled Enamel Insulated Wires Under Thermal Ageing

MUHAMMAD RAZA KHOWJA [1], **GAURANG VAKIL**[1], **(Member, IEEE),**
SYED SHAHJAHAN AHMAD[1], **RAMKUMAR RAMANATHAN**[1],
CHRIS GERADA [1,2], **(Member, IEEE), AND MAAMAR BENAROUS**[3]

[1]PEMC Research Group, University of Nottingham, NG7 2TG Nottingham, U.K.
[2]Key Laboratory of More Electric Aircraft Technology of Zhejiang Province, Ningbo 315100, China
[3]Collins Aerospace, Wolverhampton, WV10 7EH West Midlands, U.K.

Corresponding author: Muhammad Raza Khowja (Raza.Khowja@nottingham.ac.uk)

ABSTRACT This paper characterizes and develops life models for two different wire insulating materials: Poly-ether-ketone (PEEK) and nanofilled enamel (Allotherm wire). The article focuses on predicting the lifespan of PEEK and Allotherm wire insulating materials, specifically for use in low-voltage electrical machines. The study investigates the effects of thermal ageing in terms of dissipation factor, insulation capacitance, and partial discharge inception voltage (PDIV). Delamination of the insulation layer is observed in both wires during the ageing process, resulting in an increase in the differential dissipation factor and insulation capacitance. With respect to its unaged condition, Allotherm wire exhibits faster degradation, showing 2.4- and 4.5-times higher changes in the differential dissipation factor and insulation capacitance respectively compared to PEEK wire after the 16th ageing cycle. In addition, Allotherm wire experiences faster deterioration of the PDIV, with a 42% reduction compared to 32% in PEEK after the same ageing cycle. Using a single-stress Arrhenius life model, the study estimates the relative thermal index (RTI) for both materials as 245°C for PEEK and 226.25°C for Allotherm wire. These results indicate a 72.1% decrease in the lifetime of PEEK and a 25.5% decrease in the lifetime of Allotherm wire when compared to the manufacturer's RTI specification.

INDEX TERMS Dissipation factor, insulation capacitance, low voltage electrical machines, partial discharge inception voltage, thermal life, thermal index, thermal ageing, time-to-breakdown.

I. INTRODUCTION

In the recent past, the demand for sustainable and eco-friendly development has increased and electrical motors have been widely adopted as alternatives to internal combustion engines, pneumatic and hydraulic systems in automotive and aerospace applications [1]. However, the reliability of electrical machines has not been adequately verified due to which

The associate editor coordinating the review of this manuscript and approving it for publication was Yongquan Sun [id].

thermal safety factors need to be considered, resulting in over-engineering and poor power density [2].

The life of an electromagnetic device such as motor, generator, transformer, or inductor is mostly limited by the reliability of the wire insulation used in these devices. They contains several different components and features which ensure that electrical short circuit do not occur during their entire lifespan [3]. In electrical machines, the weakest insulation system is represented by the layer of inter-turn insulation, the failure of which can be penalised in terms of localised overheating within the stator. Therefore, it can trigger the

most severe motor faults (i.e., phase-to-ground and phase-to-phase) yielding to a complete power failure [4]. The stator coils in low voltage (LV) electrical machines (i.e., commonly rated for voltage less than 700Vrms) are randomly wound consisting of a thin layer of Type-I insulation (i.e., organic insulating material which can endure the effect of partial discharge). In these machines, there is the possibility of the first turn being in contact with the last turn of a coil. Therefore, characterisation of inter-turn insulation becomes an important aspect when modelling the life of Type-I insulating materials [5]. The purpose of the inter-turn insulation layer is to prevent the short circuit between the turns of a coil. If a short circuit occurs between two turns, the shorted turn will appear as secondary of transformer, leading to a large amount of circulating current flow in the faulted turn which overheats the stator windings rapidly [3].

In [2], [6], [7], and [8], the authors introduced a reliability-oriented approach based on the physics-of-failure of wire insulation. This approach aims to design electrical machines without relying on excessive safety factors, which often lead to over-engineering. This shift in concept addresses the demand for both high-power density and reliability constraints within the industrial sector. In [2] and [8], the authors conducted an investigation of turn-to-turn insulation subsystem, utilizing conventional polyamide-imide insulating material, for low voltage electrical machines. They performed accelerated thermal aging tests to establish single-stress life models for both continuous and variable duty electrical machine services. These models can be adjusted to align with the desired reliability level of a specific application. However, life models were limited to conventional polyester/polyamide-imide insulation with a thermal class of 200°C. In [9], [10], and [11], new methods have been introduced which aims at developing the life models with reduced accelerated aging test time. All three of these articles use conventional magnet wire, with a thermal class of 220°C in [9] and [10] and a thermal class of 180°C in [11]. In [9], a neural network approach is employed to predict the mean time-to-failure, where insulation resistance is considered as an end-of-life criteria i.e., measured insulation resistance is reached to a set threshold value. In [10] and [11], a curve fitting approach is used for mean life prediction, with insulation resistance (IR) and insulation capacitance (IC) serving as end-of-life criteria, respectively. While the methods outlined in [9], [10], and [11] offer faster alternatives to conventional accelerated aging tests, they come with a drawback of potential prediction inaccuracies. This level of uncertainty may not be acceptable in safety-critical industries such as aerospace, where ensuring reliability is of paramount importance.

In LV electrical machines, thermal ageing is the most dominant ageing factor which deteriorates the life of insulating material. For these machines, electrical stress is generally neglected if the motor operating voltage is less than 300V since the voltage across the insulation is well below the partial discharge inception voltage (PDIV – partial discharge inception voltage is the lowest voltage required to induce the

PD activity within the dielectric material) [2]. The primary source of thermal stress on the stator coils is due to copper losses caused by I^2R (i.e., DC resistive loss and AC proximity loss). This accelerates chemical reactions within the insulation, gradually causing the deterioration of the dielectric properties of the insulating material [12]. The thermal index of the wire insulation typically represents the maximum operating temperature that the winding of an electrical machine can withstand. As per Arrhenius law, every 8 to 10°C increase in temperature beyond the thermal index of the wire halves the insulation lifespan and vice versa [9]. To ensure an average insulation lifespan of 20,000 hours, it is common practice to design the electrical machine so that the operating temperature of the stator coils does not exceed the wire's thermal index, as defined by the wire manufacturer [9], [10]. If a longer lifespan of more than 20,000 hours is required, the design of an electrical machine needs to be modified to operate the winding temperature lower than the thermal index. However, this adversely influences the machine's torque density resulting in higher weight and volume [2]. In safety-critical applications such as aerospace, automotive and marine, the reliability requirements are much higher than those based on the manufacturer's standard life curve. This means that one cannot solely rely on the manufacturer's life curve which is typically based on 50% probability failure, ensuring a lifespan of 20,000 hours at the thermal index value. Instead, the reliability criterion for these applications typically requires a 5-10% cumulative probability of failure, which is much more stringent. To meet these requirements, the physics-of-failure methodology can be employed to develop life models at various probability percentiles. This enables machine designers to accurately predict the machine's lifespan according to the reliability needs of the given application [2], [7]. In this research paper, the authors have developed a life model for two high temperature insulated wires, namely Type-I organic Poly-ether-ketone (PEEK) and Type-II Nano-filled Enamel (Allotherm) and have compared their performance under thermal ageing. The paper is structured as follows: section II provides technical details of the materials being tested, section III explains the experimental setup for accelerated thermal ageing, section IV reports the behavior of the insulating materials with respect to thermal ageing in terms of differential tanδ, differential IC, and PDIV, section V discusses the life and breakdown data evaluation using Weibull distribution, and section VI concludes the paper.

II. INSULATING MATERIALS
A. NANOFILLER ENAMEL (ALLOTHERM)
The nanofiller enamel wire (with product name as Allotherm 602 CR Flat) is a polyamide-imide enamel wire supplied by ELANTAS based on nanotechnology to increase the partial discharge (PD) resistance. Nanofiller enamel is obtained by the homogeneous dispersion of nano-sized particles into a polymeric matrix, resulting in peculiar properties

due to the strong interaction between both the organic and inorganic polymers which are emphasized by the very large active surface of the nanometric particles. By increasing the portion of nanofillers (i.e., Corona Polyamide-imide) with the Polyester-imide (PEI) can lead to the formation of a ceramic-like layer on the coating surface which increases the resistance against PD [13], [14]. The wire is made up of a portion of 55% PEI and 45% Allotherm. Insulation thickness of the wire is $33\mu m$ with a copper core diameter of 0.8mm. The thermal index of the wire is 230°C as defined in the technical datasheet. The wire is priced at £8 per kilogram.

B. POLY-ETHER-KETONE (PEEK)

PEEK is an organic thermo-plastic polymer used as a dielectric material in the stator of electrical machines. PEEK insulated wire results from the extrusion of PEEK polymer over copper wire which is developed by ZEUS for use in challenging environments such as oil and gas, automotive, aircrafts and other electrical industries [15]. The wire is $43\mu m$ thick with a copper core diameter of 0.8mm. As per technical datasheet of the wire, the continuous operating temperature is 260°C. The cost of the wire is £176 for every kilogram.

C. ESTIMATION OF INSULATION THICKNESS

The thickness of the wire insulations (i.e., PEEK and Allotherm) is estimated through optical microscopy. The obtained cross sections of the wire were examined with an optical microscope (Olympus BX41M) in bright field mode.

The wire specimens were cold mounted in resin to obtain view polished cross sections as illustrated in Figure 1. The cut pieces of wire (approximately 2 to 3cm long) were fixed perpendicularly by using a metal clip and placed in plastic molds, which were then filled with an epoxy resin (i.e., Struers EpoFix Resin) mixed with a hardener (i.e., Struers EpoFix hardener), with a ratio of 15:2. It was left to harden for 24 hours under atmospheric pressure at room temperature to complete polymerization of epoxy resins. After removal of the wire specimens from the mold, the embedded wire was ground in a rotary motion metallurgical grinding machine with a rotating 240-grit silicon carbide paper at speed of 300 rpm using water as lubricant. Following that, the specimens were rinsed with water and ethanol to remove any remaining debris after the grinding stage.

The cross sections imaged with different objectives (i.e., from 10x to 100x). From Figure 2, the copper core and the insulating coating layer are clearly distinguishable for the wire specimen. The thickness of the insulation coating for PEEK and Allotherm wire was determined from optical microscope images taken with 100x objective which has the accuracy of about 1 micron. For each wire specimen, the insulation thickness was measured in multiple spots, where the deformation is minimal, and an average value was determined as reported in section II-A and section II-B.

III. THERMAL AGEING TEST

The accelerated thermal ageing test is performed which consists of ageing the wire specimen in the thermal chamber
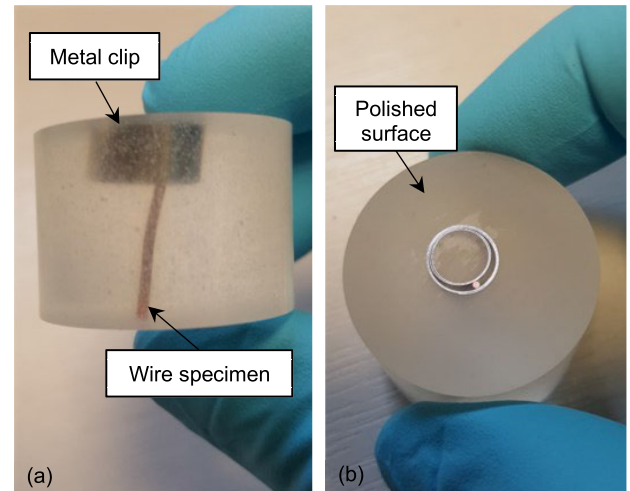

FIGURE 1. Wire specimen mounting in resin (a) side view (b) top view.

over its thermal class or thermal index. This test comprises of preparing the test specimen, measuring the diagnostic properties, ageing the specimens thermally and calculating the time-to-breakdown, the details of which are discussed in the following subsections.

A. TEST SPECIMEN

The test specimen is a twisted pair which is made up of two identical parallel insulated wires held in hand twisted together to form a single specimen as shown in Figure 3. The length of each twisted pair specimen is approximately 200mm with 8 full 360° twists. The force acting on the specimen is 13N. The specimen holder is equipped with 10 unaged twisted pair specimens for each thermal exposure without the application of resin or impregnation. All the specimens were prepared as per technical standards ASTM D2307 and IEC 60034-18-31 [16], [17].

B. TEST PROCEDURE

Accelerated ageing test is performed which is commonly used for thermal qualification of wire insulating material [16], [17]. The specimens of both insulating materials are thermally aged above thermal index of the wire, as defined by the wire manufacturer, in a repeated cycle until the inter-turn short circuit is detected in each specimen. The ageing was carried out in a controlled oven (CARBOLITE GERO) whose maximum temperature rating is 400°C, with tolerance of ±0.1%. The ageing temperatures for both PEEK and Allotherm wires considered to be the same which are 270°C, 290°C and 310°C. The corresponding diagnostic cycle for PEEK wire is 144, 40 and 10 hours and for Allotherm wire is 72, 20 and 5 hours at ageing temperature 270°C, 290°C and 310°C respectively.

C. WIRE DIAGNOSIS

In terms of diagnosis of the insulating material under test, dissipation factor (Tanδ) and insulation capacitance (IC) is measured after each thermal cycle. This is carried out with the
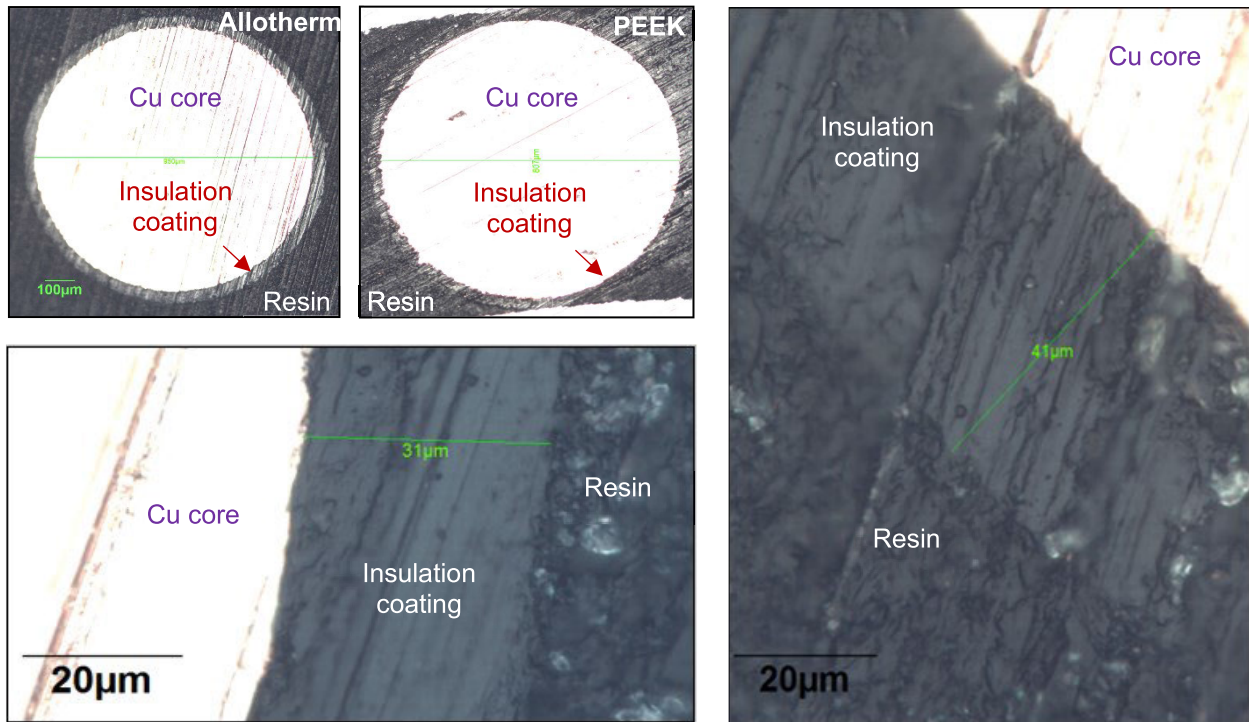
FIGURE 2. Optical microscopy of PEEK and Allotherm wires.

help of MEGGER Delta 4000 Device as shown in Figure 3. MEGGER performs an "AC Hipot Test" in which ramp voltage is applied across the insulating material (i.e., inter-turn insulation in this paper) up to the predefined voltage and measure Tanδ and IC. This predefined voltage is typically set close to the PD inception voltage of the material for the unaged specimens. This maximum voltage was kept constant under thermal ageing with a maximum RMS voltage stress of 720V and 630V across the insulation of PEEK and Allotherm wire specimens respectively, lasting for about 2 minutes. When a short circuit is detected in a specimen time-to-breakdown was noted down until the failure is detected in each specimen. The entire thermal ageing process is depicted in Figure 4. During the whole ageing test procedure, the ambient temperature and relative humidity were kept under 25°C and 40% respectively.

IV. DEGRADATION UNDER THERMAL AGEING

The degradation of insulating materials (PEEK and Nanofiller enamel insulated wires) under thermal ageing is investigated. The diagnostic properties of dielectric material such as Tanδ, IC and PDIV have been measured. These results are helpful to assess the condition of the insulating material over the ageing period.

A. TANδ AND IC

The Tanδ and IC tests are commonly used together to provide a comprehensive assessment of the quality of the dielectric material used in electrical machines. The Tanδ test measures

FIGURE 3. 10 twisted pair specimens and their diagnosis via MEGGER.

the dielectric losses, which can indicate the presence of defects, moisture or any other contamination that can reduce the quality of insulating material. A high Tanδ implies that
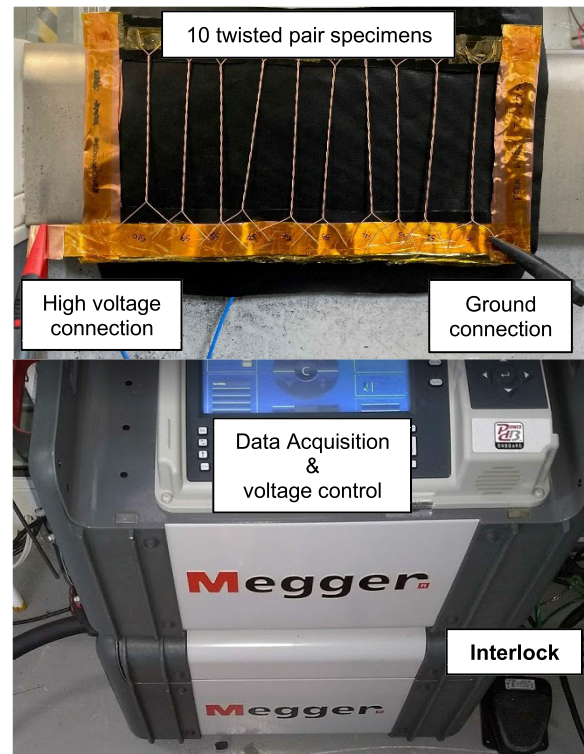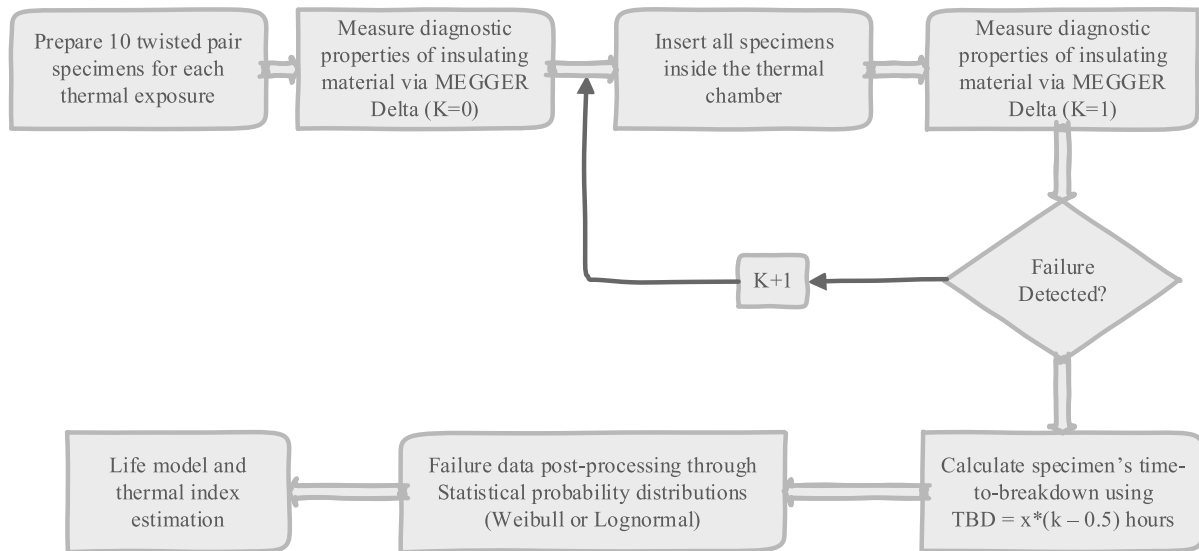
FIGURE 4. Complete thermal ageing and life test procedure.

the material has high losses and may not be able to provide enough insulation for the intended application.

The IC test measures the ability of the material to store electrical charge. It can potentially identify the defects within the insulation, such as cracks or voids, which can reduce the capacitance of the dielectric material. For E.g., a low value of IC can indicate the presence of defects or contaminants that can reduce the dielectric strength of the material and increase the risk of electrical breakdown [3], [18]. On the other hand, it has been reported that the IC of a dielectric material can increase under thermal ageing phenomenon due to the de-polymerization and oxidation byproducts. This can increase the permittivity of dielectric material and hence can contribute to increase capacitance [19], [20], [21]. Depolymerization is the process by which a polymer breaks down into smaller molecules. This can occur due to exposure to heat or chemical reactions, and can result in the formation of depolymerization by-products, which are smaller molecules that can deteriorate the dielectric properties. Oxidation byproducts, on the other hand, are compounds that are formed when polar compounds in dielectric material react with oxygen. Both depolymerization and oxidation by-products can affect the long-term performance of insulating material, leading to reduced electrical properties such as PDIV, breakdown voltage and dielectric strength [19], [22].

Figure 5a and Figure 5b show the Tanδ and IC of PEEK insulated wire whereas Tanδ and IC of Allotherm wire are illustrated in Figure 6a and Figure 6b, with respect to the test voltage and thermal ageing cycles. From Figure 5a and Figure 6a, two major changes in the dissipation factor can be noticed – one is the rate of change dissipation factor at low voltage and the other is dissipation factor at voltage above the PDIV. The change in the dissipation factor at low voltage (i.e., under thermal ageing) represents the polarization and

conduction losses within the insulation whereas the change in dissipation factor at voltage higher than PDIV, may be the indication of delamination effect (i.e., the layer of insulation comes off the copper conductor with increase in thermal ageing cycles), which results in higher PD activity. From unaged to 16th thermal ageing cycle, the change in dissipation factor (i.e., at voltage lower than PDIV) of Allotherm wire is approximately two times higher than PEEK insulated wire. This is the indication of higher polarisation and conduction losses in Allotherm wire. With reference to unaged value, the rate of change of dissipation factor is also compared, for both PEEK and Allotherm wires, at 690V and 630V respectively. This gives rise to the dissipation factor of 18.3% and 43.2% respectively, going from unaged to 16th ageing cycle. This suggests that the ionization of air-filled voids in PEEK insulated wire is lower, resulting in lower PD activity and higher PDIV, when compared with Allotherm wire.

The variation in IC (i.e., lower than PDIV) as a function of thermal ageing is depicted in Figure 5b and Figure 6b. For PEEK insulated wire, IC is monotonically decreasing under thermal ageing. With reference to the unaged specimens, at voltage lower than PDIV, IC is reduced by 20% whereas non-monotonic trend is noticed for Allotherm wire. For Allotherm wire the IC is increased, from unaged to 8th ageing cycle. This could be due to the higher polar ageing byproducts for the aged specimens until 320 hours (i.e., 8th ageing cycle) releasing higher permittivity. Subsequently, after the 8th ageing cycle, IC decreases notably which can be attributed to the transformation of some polar compounds in the thermally aged specimens into non-polar ones [19] This results in lower permittivity which is evident from the 8th ageing cycle to the 16th ageing cycle. At the maximum diagnostic voltage (i.e., 690V for PEEK and 630V for Allotherm), the IC is reduced by 5.9% in PEEK specimens whereas reverse
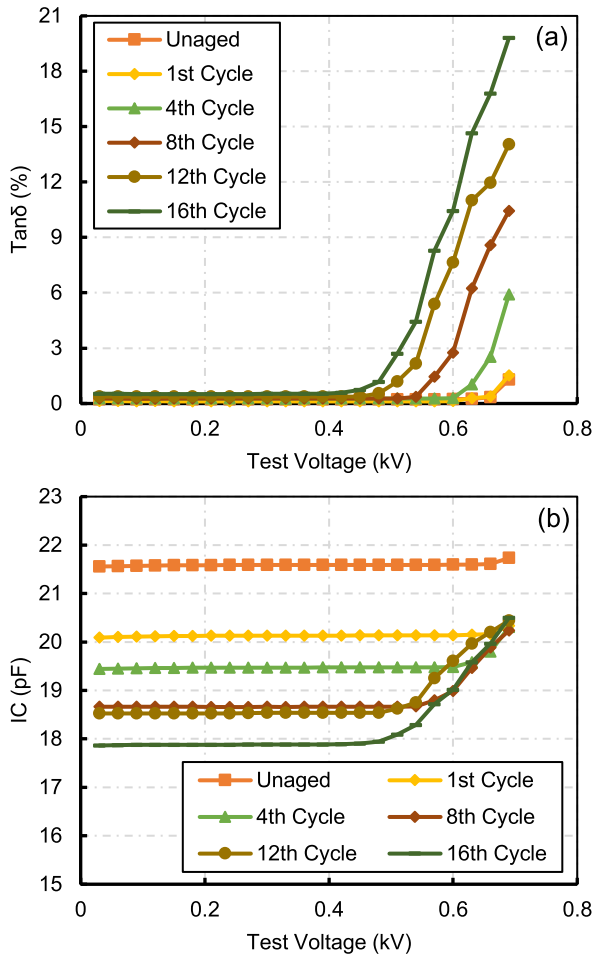
FIGURE 5. Measurement results of PEEK wire at 290°C (a) mean dissipation factor of ten twisted pair specimens (b) mean insulation capacitance of ten twisted pair specimens.
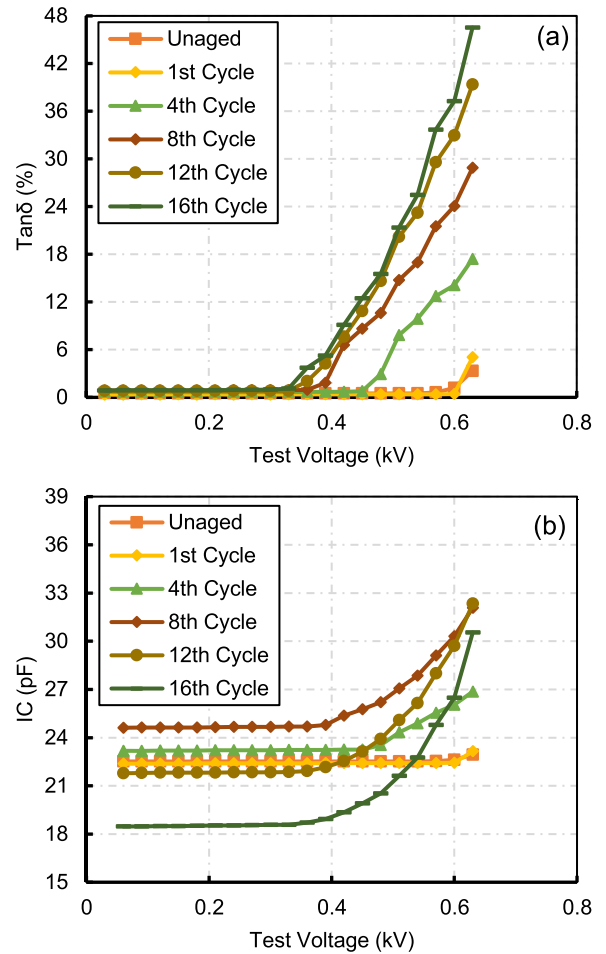

FIGURE 6. Measurement results of Allotherm wire at 290°C (a) mean dissipation factor of ten twisted pair specimens (b) mean insulation capacitance of ten twisted pair specimens.

holds for Allotherm wire, increasing IC by 25% with respect to the unaged condition.

B. △TANδ AND △IC

The differential dissipation factor ($\Delta tan\delta$) and the differential insulation capacitance (ΔIC) of PEEK and Allotherm wires under thermal ageing has been investigated in this section. As stated in the previous section, after every ageing cycle insulation health is assessed in terms of dissipation factor and IC with respect to the ramp voltage applied across the inter-turn insulation. Figure 4 and Figure 5 illustrate the $\Delta tan\delta$ and ΔIC which has resulted from the Tanδ and IC measurement via MEGGER Delta by using (1) and (2).

$$\%\Delta Tan\delta = \%Tan\delta_{hv} - \%Tan\delta_{lv} \qquad (1)$$

$$\%\Delta IC = 100 * \left(\frac{IC_{hv} - IC_{lv}}{IC_{lv}} \right) \qquad (2)$$

The "lv" and "hv" subscripts are used for low and high voltage respectively. The lv is measured at 30V for both PEEK and Allotherm wires whereas, hv is measured at 690V and 630V for PEEK and Allotherm wires respectively. For

the sake of fair comparison between both the wires, the value of hv is chosen equal to the PDIV value (i.e., mean value of all ten specimens) measured on unaged specimens. From Figure 7 and Figure 8, it is evident that there is a rising trend in $\Delta tan\delta$ and ΔIC with respect the thermal ageing cycles (i.e., from unaged to the aged 16th cycle). In comparison to its unaged condition, at 16th ageing cycle, the $\Delta tan\delta$ and ΔIC in Allotherm wire is increased by a significant margin, delivering 2.4 and 4.5 times higher $\Delta tan\delta$ and ΔIC than PEEK. When comparing the dielectric performance of both wires, it is evident that the Allotherm wire loses its dielectric properties faster than the PEEK wire under thermal ageing throughout the ageing process. Based on the variations in $\Delta tan\delta$ and ΔIC, which have also been reported in [18] for other dielectric materials, the following findings can be made.

- The rate of change in size and number of air-filled voids is reduced in PEEK since the change in dissipation factor gets smaller during thermal ageing.
- The delamination effect in Allotherm wire is faster than PEEK insulated wire.
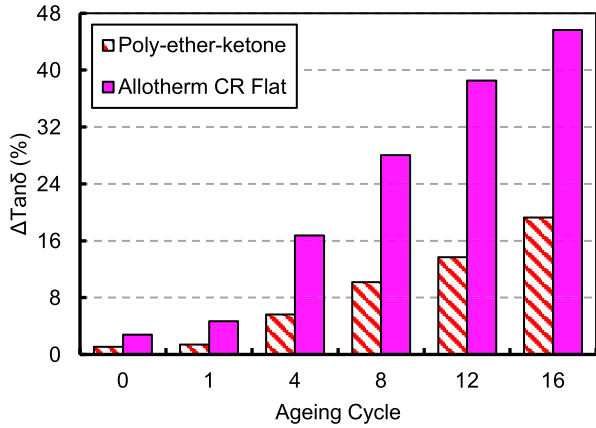
FIGURE 7. Differential Tanδ for PEEK and Allotherm Wires, resulting from the Tanδ measurement via MEGGER Delta 4000.

FIGURE 8. Mean Differential IC for PEEK and Allotherm Wires, resulting from the IC measurement via MEGGER Delta 4000.
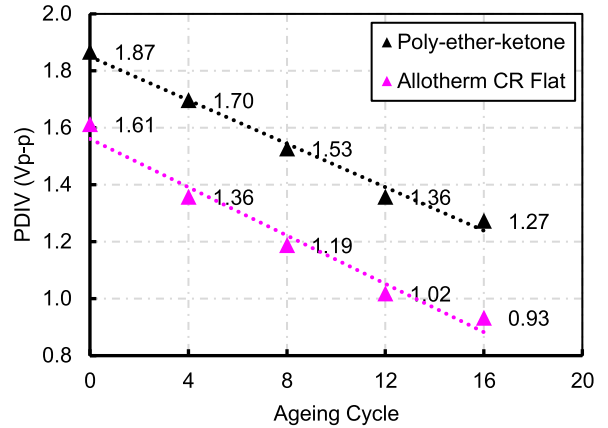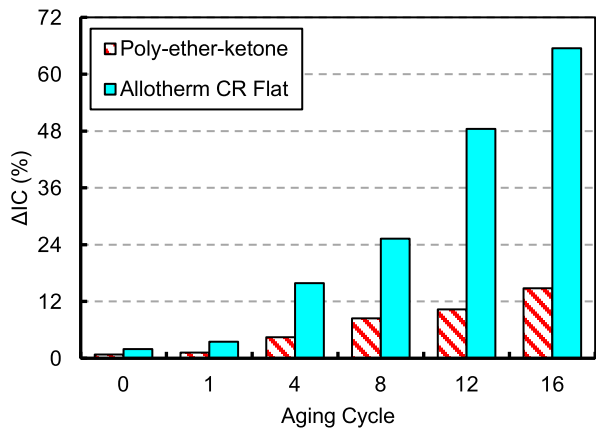

FIGURE 9. PDIV obtained from Tanδ measurement, under the application of AC ramp voltage. Mean of all ten specimens at T2.
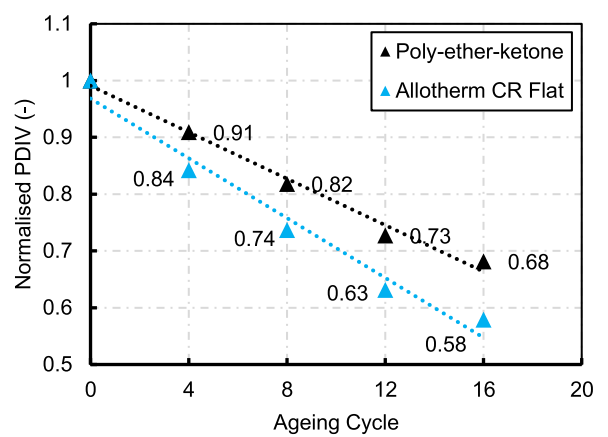

FIGURE 10. Normalised PDIV obtained from Tanδ measurement, under the application of AC ramp voltage, Mean of all ten specimen at T2.

• With respect to unaged specimens, higher rate of change of Δtanδ and ΔIC refers to the greater energy consumed by PD.

C. PDIV

PDIV, also referred to as partial discharge inception voltage, is the minimum voltage at which partial discharge starts to occur in a dielectric material. This PD activity can bridge the air-filled voids in the material, leading to the degradation of the insulation performance and eventually the breakdown of the electrical system made with Type-I insulation [2], [5]. The PDIV of a given material defines the quality and performance of insulation which can be negatively impacted by thermal ageing, increasing the risk of PD activity for several reasons:

• **Changes in the material properties –** Thermal ageing can cause changes in the physical and chemical properties of insulating materials, including the permittivity, conductivity, and mechanical strength. These changes can lead to a breakdown of the insulation material, increasing the risk of PD.

• **Formation of defects –** Thermal ageing can also result in the formation of defects within the insulation material, such as voids, cracks, and delamination. These defects

can act as partial discharge initiation sites and can lead to the breakdown of the insulation material.

• **Increased polarisation –** Thermal ageing can cause an increase in the polarisation of the insulation material, resulting in space charge accumulation that can lead to initiating PD activity.

• **Presence of by-products –** During thermal ageing, the insulating material can degrade and produce by-products such as gases, free radicals, and polar compounds. These by-products can act as partial discharge initiation sites and increase the risk of partial discharge.

Therefore, it is important to examine the condition of insulation and take appropriate steps to prevent electrical breakdown where it is needed the most. For example, in aerospace applications, medium voltage electrical machines constructed with Type-I insulation that operate at low pressure are more prone to PD activity, which compromises their reliability and increases the need for appropriate prevention measures.

The PDIV is determined from the dissipation factor method [23], also known as indirect method of determining PDIV, as a function of thermal ageing cycles for both PEEK and Allotherm wires as reported in Figure 9. In Figure 10, the PDIV values are normalised with respect to their unaged

values. It is worth noting that the PDIV should be measured using direct methods such as UHF antenna or photomultiplier when modeling the life and assessing the condition of the insulation in high voltage applications. Since this paper targets low voltage electrical machines, where the PDIV is not a breakdown criterion (i.e., the PDIV is well below the motor operating voltage), it is reasonable to observe and compare the PDIV using an indirect method such as dissipation factor or insulation capacitance measurements via MEGGER [5], [19]. From Figure 9, it can be observed that the PDIV of the PEEK wire is 1.16 times higher than the PDIV of Allotherm wire when specimens are not thermally aged. This may be due to the 10μm difference in their insulation thickness. Nevertheless, this results in similar values of electrical strength in kV/mm. The behavior of the insulation as a function of thermal ageing can be predicted by the normalized PDIV. In Figure 10, the PDIV in the Allotherm wire deteriorates at a much faster rate compared to the PEEK wire. After the 16th ageing cycle, the PDIV reduction in the Allotherm wire is approximately 42%, while in the PEEK wire it is about 32%. This may be due to the faster delamination of the Allotherm insulation under thermal ageing, resulting in more voids that cause PD to occur at a faster rate than in the PEEK wire. The relationship of PDIV with respect to ageing time (in hours) under thermal exposure T2 (i.e., 290°C) can be drawn from Figure 9 and Figure 10. Equations (3) and (4) can be used to obtain the PDIV relation for PEEK and Allotherm, respectively.

$$PDIV_{Peek} = 1.850 - 0.00382t \quad (3)$$

$$PDIV_{Allotherm} = 1.561 - 0.00848t \quad (4)$$

D. AGED SPECIMENS

The condition of each twisted-pair specimen of both PEEK and Allotherm wires is observed after the breakdown is detected in all the specimens. Figure 11 and Figure 12 show three specimens of each wire, pointing out the severity of the delamination effect in both wires. It is evident that the color of the specimens has changed due to exposure to high temperature. Moreover, both insulating materials are partly damaged and lose their mechanical strength with thermal ageing. However, the delamination effect observed in Allotherm wire is relatively higher than in PEEK, as confirmed by visual inspection. In other words, the PEEK insulation remains intact on the copper surface, whereas the Allotherm wire insulation becomes brittle which separates from the conductor upon contact. The validation of this can be further confirmed by examining the variation in insulation capacitance (i.e., IC and ΔIC) illustrated in Figure 5b, Figure 6b and Figure 8.

V. TIME-TO-BREAKDOWN

The breakdown or failure time of each specimen has been collected and post-processed with the help of two-parameter Weibull probability distribution. The Weibull distribution is widely used in statistical analysis to process data obtained

TABLE 1. Weibull parameters for PEEK wire.

Ageing Temperature	Scale, α	Shape, β	L$_{(P50)}$
270°C	2233.1	11.89	2165
290°C	731.2	16.02	715
310°C	116.4	6.23	111

TABLE 2. Weibull parameters for Allotherm wire.

Ageing Temperature	Scale, α	Shape, β	L$_{(P50)}$
270°C	866.0	6.81	806
290°C	257.3	18.32	250
310°C	75.1	3.19	67

from accelerated lifetime tests. One of its key advantages is its capability to model failure rates that can either increase, decrease or constant failure rates. The specific formulation of the cumulative distribution function F(t) can be found in equation (5) [24]. The parameter t represents the Time-to-Breakdown of the specimens after a short-circuit fault is detected between the layers of insulation. α, referred to as the scale parameter, represents 63.2% of the insulation lifetime. On the other hand, the parameter β, known as the shape parameter, determines the slope of the Weibull distribution.

$$F(t) = 1 - e^{-\left(\frac{t}{\alpha}\right)^{\beta}} \quad (5)$$

The Time-to-Breakdown of each specimen under all three all three thermal exposures are plotted and depicted in Figure 13 and Figure 14, and the specific distribution parameters can be found in detail in Table 1 and Table 2. The Time-to-Breakdown for each specimen in the test is determined when the specimen fails the AC hipot test. The actual Time-to-Breakdown is then calculated by subtracting the half duration of the last ageing cycle from the total thermal exposure duration. The mean life, L$_{(P50)}$, is determined by extracting the lifetime at 50% probability failure from the Weibull distribution, to compare the thermal index defined by the wire supplier. Nevertheless, different failure percentiles can be obtained to meet the reliability needs, For E.g., a recommended range of 1% to 5% failure probability is suggested for aerospace applications, and 5% to 10% for automotive applications [2].

VI. LIFE MODEL

The thermal life of solid insulating material can be determined using equation (6), where the insulation constants A and B are derived from experimental failure data, and L represents the thermal life of the insulating material in hours at the operating temperature T in Kelvin.

$$L = Ae^{B/T} \quad (6)$$

If the electrical ageing is neglected, the thermal life of insulating material can be determined using equation (6) and

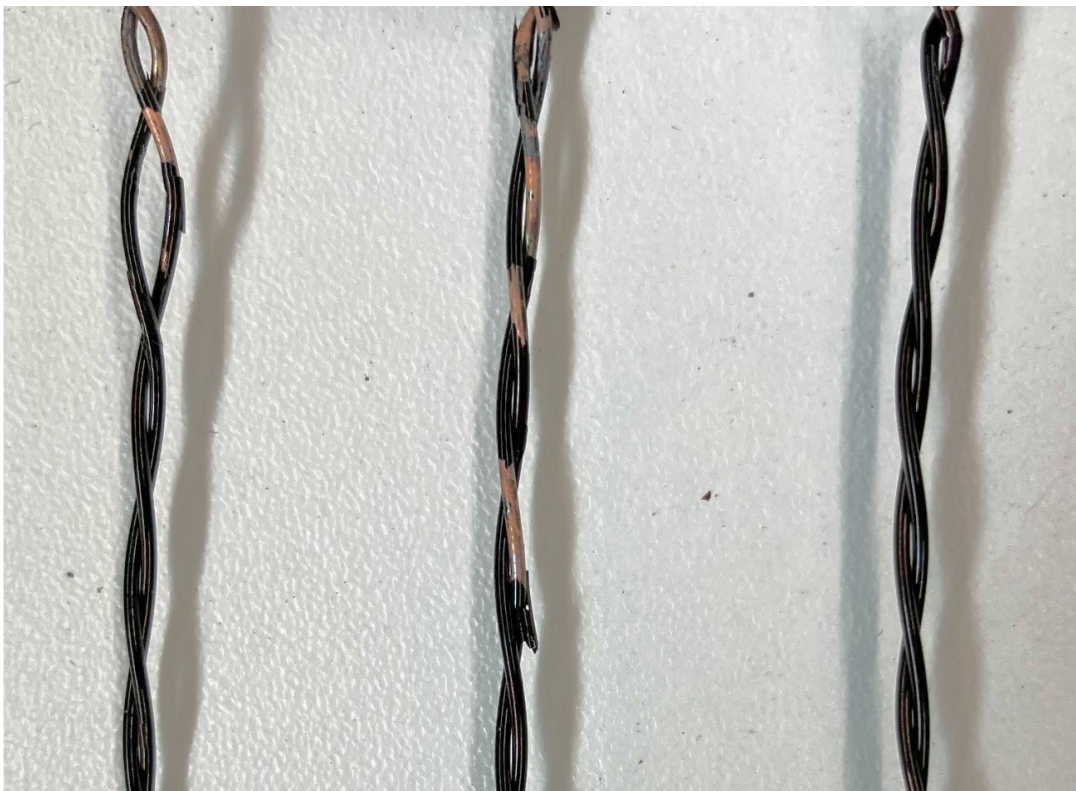**FIGURE 11.** Observation of PEEK wire specimens.

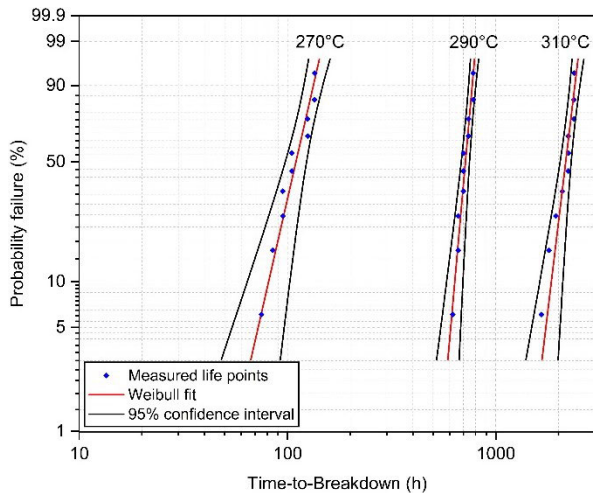**FIGURE 12.** Observation of Allotherm wire specimens.

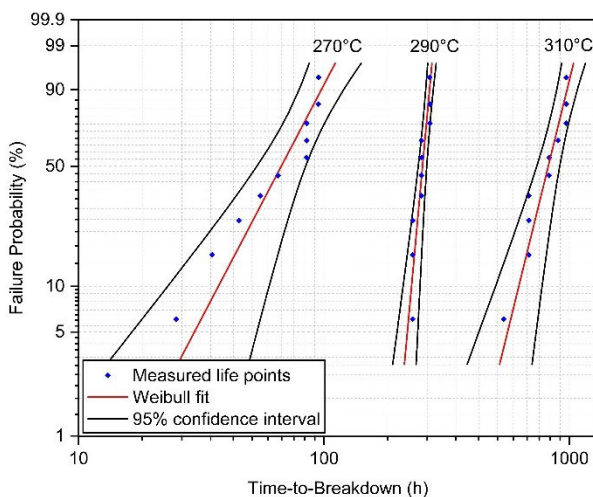**FIGURE 13.** Weibull distribution plot for PEEK at 270°C, 290°C & 310°C.

FIGURE 14. Weibull distribution plot for Allotherm at 270°C, 290°C & 310°C.

linearized by taking the logarithm on both sides. The resulting equation, denoted by (7),

$$log_{10}L = \log_{10}A + (log_{10}e).\frac{B}{T} \tag{7}$$

(7), represents the life of the insulating material as a straight-line equation with B' as the slope and A' as the y-intercept.

Thermal stress plays a dominant role in the gradual degradation of insulating material in low voltage electrical machines since the effects of electrical ageing in these machines are often disregarded or ignored. This leads to insulation failure which can eventually result in permanent breakdown if timely maintenance is not conducted. It is essential to evaluate the insulation system's ability to withstand thermal ageing. The primary source of thermal stress in electrical machines is the heat generated in the stator due to

hysteresis effect and eddy currents in the stator steel, as well as I^2R losses in the copper wire. Operating a stator at high temperature triggers a chemical reaction through oxidation, making the insulating material brittle. Additionally, it can lead to the delamination of the insulation layer, resulting in a loss of bonding strength and resin impregnation compound [3], [9]. Under accelerated ageing, the deterioration process follows a first-order chemical reaction, with the reaction rate governed by the Arrhenius law proposed by Dakin in 1971 [9], [25].

Equation (7) can be further expressed in the form of equation (8).

$$Y = A' + B'X \tag{8}$$

$Y = \log_{10}L$
$A' = \log_{10}A$
$X = 1/T$
$B' = (\log_{10}e). B$

To obtain the constants A' and B', experimental data from accelerated thermal ageing tests can be used along with the least square method. The constants A' and B' can be calculated using equations (9) and (10) respectively.

$$A' = \frac{\sum Y - B'\sum X}{N} \tag{9}$$

$$B' = \frac{N\sum XY - \sum X\sum Y}{N\sum X^2 - (\sum X)^2} \tag{10}$$

The number of ageing temperatures considered in the accelerated ageing test is denoted by N. Once the constant A' and B' are determined, the relative thermal index at a life of 20,000 hours can be determined as shown in equation (11). The correlation coefficient "R", which indicates the goodness of fit of the curve to a linear regression line, can be calculated using equation (12).

$$RTI = \frac{B'}{4.301 - A'} - 273 \tag{11}$$

$$R = \sqrt{\frac{A'\sum Y + B'\sum XY - N(Y_{avg})^2}{\sum Y^2 - N(Y_{avg})^2}} \tag{12}$$

The most vulnerable part of the electrical machine's insulation is the occurrence of a turn-to-turn short circuit fault. If this fault is not addressed, it can result in a short circuit between phases or to the ground, depending on the winding configuration [2], [5], [9], [26]. Therefore, the study presented in this article focuses on low voltage electrical machines (i.e., where electrical stress is ignored) to develop a life model specifically for turn-to-turn short circuit faults. The mean life, $L_{(P50)}$, which was determined in the previous section, is extrapolated using the least square method, as indicated by equations (7) to (12). Figure 15 shows the insulation life with respect to temperature for both PEEK and Allotherm wire. The corresponding model calculations can be found in Table 3 and Table 4, while the life model constants are listed in Table 5. The measured life points align well with

TABLE 3. Life model calculation for PEEK wire.

	Temperature in °C	Temperature in K	X = 1/T	X-square	$L_{(p50)}$ (h)	Y = Log_{10}L	XY = $(Log_{10}$L)/T	Y-square
1	270	543	0.001842	3.39E-06	2165	3.33546	0.00614	11.13
2	290	563	0.001776	3.15E-06	715	2.85431	0.00507	8.15
3	310	583	0.001715	2.94E-06	111	2.04532	0.00351	4.18
N = 3	3	3	ΣX = 0.00533	ΣX^2 = 9.49e-6		ΣY = 8.24	ΣXY = 0.01472	ΣY^2 = 4.18

TABLE 4. Life model calculation for Allotherm wire.

	Temperature in °C	Temperature in K	X = 1/T	X-square	$L_{(p50)}$ (h)	Y = Log10L	XY = (Log10L)/T	Y-square
1	270	543	0.001842	3.39E-06	806	2.90634	0.00535	8.45
2	290	563	0.001776	3.15E-06	250	2.39794	0.00426	5.75
3	310	583	0.001715	2.94E-06	67	1.82607	0.00313	3.33
N = 3	3	3	ΣX = 0.00533	ΣX^2 = 9.49e-6		ΣY = 7.13	ΣXY = 0.01274	ΣY^2 = 17.53

TABLE 5. Life model constants and thermal index.

PARAMETERS	A'	B'	*ETI	+MTI	R	R-squared
PEEK Wire	-15.340	10175.42	244.97°C	260°C	0.986	0.973
Allotherm Wire	-12.804	8539.88	226.25°C	230°C	0.999	0.997

*ETI = Estimated Thermal Index   +MTI = Manufacturer Thermal Index

the equation of a straight line with a correlation coefficient (R) very close to 1, as illustrated in Table 5. This indicates a strong correlation and demonstrates the effectiveness of the thermal life curve fitting for both PEEK and Allotherm wires. The regression line, calculated using equation (7), is extended to a lifetime of 20,000 hours, representing the relative thermal index (RTI) of the wire. This RTI is displayed as a dotted line in Figure 15 which serves as a standardized parameter defined by wire manufacturers for their customers. The RTI for both wires is calculated using equation (11) and then compared with the RTI specified by the manufacturers. The temperature difference between the estimated thermal index and the manufacturer's thermal index is found to be 15°C for PEEK wire and 3.75°C for Allotherm wire. This results in a percentage error of 5.76% for PEEK wire and 1.63% for Allotherm wire. The RTI value for Allotherm wire aligns well with the RTI defined by the wire manufacturer, indicating a good agreement. However, a noticeable percentage error is observed for PEEK wire. It is worth noting that the supplier of the PEEK wire has specified a continuous operating temperature of 260°C but has not explicitly stated it as the RTI. Hence, in this article, the authors have assumed that this temperature of 260°C represents the wire's thermal index for the purpose of conducting a comparative study, where the insulation's lifetime is set at 20,000 hours. In addition, by utilising the life curve displayed in Figure 15, it is possible to determine the insulation life at RTI specified by wire manufacturers. This calculation yields a lifespan of 5,586 hours for PEEK wire and 14,906 hours for Allotherm wire. It is notable that even slight changes in operating temperature (precisely 15°C for PEEK wire and 3.75°C for Allotherm wire) can lead to significant differences in the required lifespan, considering that the manufacturer sets a standard shelf life of 20,000 hours.

Consequently, this has resulted in a degradation of 72.1% in the lifespan of PEEK wire and 25.5% in the lifespan of Allotherm wire, when compared to the standard 20,000-hour shelf life.

VII. APPLICATION AND COST PERSPECTIVE

In safety-critical applications, such as aerospace, automotive, and marine industries, the reliability requirements are significantly more stringent than those defined by the manufacturer's standard life curve. This implies that the designer cannot solely depend on the manufacturer's life curve, which is typically derived from 50% probability failure data (or arithmetic mean of time-to-breakdown) and guarantees a lifespan of 20,000 hours at a given thermal index value. However, for these applications, the reliability criteria typically demand a 5-10% cumulative probability of failure, which is significantly more rigorous. his can be achieved by extracting the insulation lifetime (i.e., time-to-breakdown as depicted in Figure 13 and Figure 14) at a specified failure probability percentile, typically between 1% and 50%, to build the life model. This will enable the E-machine designer to make precise predictions regarding the machine's lifespan in accordance with the reliability requirements of the given application.

The lifespan of an electrical machine primarily depends on the reliability of its insulation system. To meet industry standards, electrical machines are typically subjected to qualification processes outlined in technical standards like IEC 60034 18-21 and IEEE Std. 117-2015 prior to being introduced to the market. It is important to note that the study described in this article does not aim to replace these standards, which must be followed by manufacturers when required [9], [10]. Rather, the focus of this research is mainly

directed towards researchers, with the objective of developing thermal life models that can be used during the initial stages of prototyping for low voltage electrical machines, thereby meeting the reliability needs. Traditionally, reliability requirements have been met through over-engineering, where safety factors are applied based on experience and general guidelines. However, this conventional approach, lacking specific life models, often results in lower power density as the full thermal capacity of the insulation materials is not fully utilised. To address this challenge, a shift from performance-oriented design to reliability-oriented design is necessary. This entails considering reliability right from the initial design stage and employing the developed lifetime models presented in this article, by adopting the physics-of-failure approach [2], [9].

It is important to note that although the Type-II insulating material is typically employed in medium to high-voltage electrical machines, the main objective of this paper was to evaluate the thermal performance and conduct a comparative analysis between Type-I and Type-II insulating materials specifically solely from the perspective of thermal ageing. Additionally, it should be noted that in applications where electrical ageing plays a more significant role than thermal ageing, Type-II insulation is expected to outperform Type-I insulation. Future publications will discuss the behavior of PEEK and Allotherm wires under the combined effects of thermal and electrical ageing, with a specific emphasis on PDIV as an end-of-life criterion. This is in contrast to the approach taken in this article, which uses the AC Hipot test as the method for end-of-life evaluation.

From a cost perspective, despite PEEK wire having a longer lifespan than Allotherm wire, the cost of PEEK (£176 per kg) is not justified, especially when Allotherm wire is available at a much lower cost of £8 per kg. In applications where cost is a significant factor, opting for Allotherm wire may be more reasonable than PEEK. However, this decision comes with a trade-off in power density requirements, as electrical machines using Allotherm wire need to be designed for operation at 226°C, compared to 245°C for PEEK wire (for a 20,000 hours lifespan). Consequently, if electrical machines with PEEK wire operate at the same temperature as those with Allotherm wire (i.e., at 226°C), there would be a lifespan difference of roughly 80,000 hours (refer to Figure 15).

VIII. CONCLUSION

Traditionally, the design approach to design electrical machines has been primarily focused on performance, often neglecting reliability as a key design objective. This has led to excessive over-engineering and reliance on safety factor assumptions, resulting in compromised power density within the motor drive system. However, this article takes a progressive approach by developing life models that are based on accelerated thermal ageing processes. This enables a more accurate understanding of insulation degradation and facilitates the optimal utilisation of insulating materials,
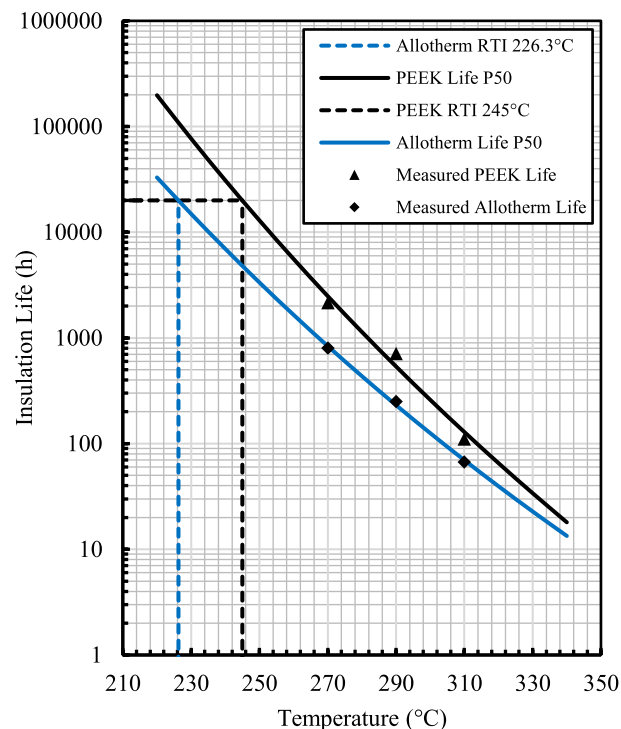

FIGURE 15. Life curve of PEEK and Allotherm wires at 50% probability.

ensuring a satisfactory level of reliability without the need of using unnecessary safety factors. This article predicts the lifespan of two wire insulating materials, namely PEEK and nanofilled enamel (Allotherm wire), with a specific focus on low voltage electrical machines. Throughout the life testing process, the impact of thermal ageing was examined by measuring the dissipation factor, insulation capacitance, and partial discharge inceptions. Additionally, the aged specimens of both PEEK and Allotherm wires were observed under a microscope to further investigate their condition. For both the wires, the investigation has shown that there is a consistent relationship between thermal ageing and the differential dissipation factor and insulation capacitance. This observation indicates that the insulation coating tends to undergo delamination during the ageing process. In relation to the unaged condition, following the 16th ageing cycle, the $\Delta\tan\delta$ and ΔIC in Allotherm wire exhibited a substantial increase, with Allotherm specimens delivering 2.4 and 4.5 times higher $\Delta\tan\delta$ and ΔIC compared to PEEK specimens. This indicates that Allotherm wire lost its dielectric properties faster than the PEEK wire during the thermal ageing process. In terms of partial discharge inception voltage (PDIV), Allotherm wire deteriorated at a much faster rate compared to the PEEK wire. After the 16th ageing cycle, the PDIV reduction in the Allotherm wire was about 42%, while in the PEEK wire it was about 32%. This may have been due to the faster delamination of the Allotherm coating under thermal ageing, resulting in more voids that caused PD to occur at a faster rate than in the PEEK wire. Furthermore, a single-stress life model was developed to determine the

relative thermal index (RTI) of the insulating materials. The mean life, $L_{(P50)}$, was obtained from the Weibull probability distribution, utilizing a 95% confidence interval at the 50th percentile. A comparison was made between the RTI of both PEEK and Allotherm wires and the RTI specified by the wire manufacturer. The estimated RTI values for PEEK and Allotherm wires were found to be 245°C and 226.25°C, respectively. These estimations resulted in a decrease in the wire lifetime by 72.1% for PEEK and 25.5% for Allotherm wire when compared to the manufacturer's RTI.

REFERENCES

[1] M. R. Khowja, G. Vakil, C. Gerada, T. Yang, S. Bozhko, and P. Wheeler, "Trade-off study of a high power density starter-generator for turboprop aircraft system," in *Proc. IECON 45th Annu. Conf. IEEE Ind. Electron. Soc.*, vol. 1, Oct. 2019, pp. 1435–1440, doi: 10.1109/IECON.2019.8926961.

[2] P. Giangrande, V. Madonna, S. Nuzzo, and M. Galea, "Moving toward a reliability-oriented design approach of low-voltage electrical machines by including insulation thermal aging considerations," *IEEE Trans. Transport. Electrific.*, vol. 6, no. 1, pp. 16–27, Mar. 2020.

[3] G. C. Stone, E. A. Boulter, I. Culbert, and H. Dhirani, *Electrical Insulation for Rotating Machines: Design, Evaluation, Aging, Testing, and Repair.* Hoboken, NJ, USA: Wiley, 2004.

[4] V. Madonna, P. Giangrande, L. Lusuardi, A. Cavallini, C. Gerada, and M. Galea, "Thermal overload and insulation aging of short duty cycle, aerospace motors," *IEEE Trans. Ind. Electron.*, vol. 67, no. 4, pp. 2618–2629, Apr. 2020, doi: 10.1109/TIE.2019.2914630.

[5] V. Madonna, P. Giangrande, W. Zhao, H. Zhang, C. Gerada, and M. Galea, "Electrical machines for the more electric aircraft: Partial discharges investigation," *IEEE Trans. Ind. Appl.*, vol. 57, no. 2, pp. 1389–1398, Mar. 2021.

[6] P. Giangrande, V. Madonna, and M. Galea, "Reliability oriented design of low voltage electrical machines based on accelerated thermal aging tests," in *Proc. Int. Symp. Power Electron., Electr. Drives, Autom. Motion (SPEEDAM)*, Jun. 2020, pp. 448–453, doi: 10.1109/SPEEDAM48782.2020.9161974.

[7] V. Madonna, P. Giangrande, and M. Galea, "Introducing physics of failure considerations in the electrical machines design," in *Proc. IEEE Int. Electric Mach. Drives Conf. (IEMDC)*, May 2019, pp. 2233–2238, doi: 10.1109/IEMDC.2019.8785304.

[8] M. Galea, P. Giangrande, V. Madonna, and G. Buticchi, "Reliability-oriented design of electrical machines: The design process for machines' insulation systems MUST evolve," *IEEE Ind. Electron. Mag.*, vol. 14, no. 1, pp. 20–28, Mar. 2020, doi: 10.1109/MIE.2019.2947688.

[9] G. Turabee, M. R. Khowja, P. Giangrande, V. Madonna, G. Cosma, G. Vakil, C. Gerada, and M. Galea, "The role of neural networks in predicting the thermal life of electrical machines," *IEEE Access*, vol. 8, pp. 40283–40297, 2020, doi: 10.1109/ACCESS.2020.2975985.

[10] M. R. Khowja, G. Turabee, P. Giangrande, V. Madonna, G. Cosma, G. Vakil, C. Gerada, and M. Galea, "Lifetime estimation of enameled wires under accelerated thermal aging using curve fitting methods," *IEEE Access*, vol. 9, pp. 18993–19003, 2021.

[11] V. Madonna, P. Giangrande, G. Migliazza, G. Buticchi, and M. Galea, "A time-saving approach for the thermal lifetime evaluation of low-voltage electrical machines," *IEEE Trans. Ind. Electron.*, vol. 67, no. 11, pp. 9195–9205, Nov. 2020, doi: 10.1109/TIE.2019.2956378.

[12] V. Madonna, P. Giangrande, and M. Galea, "Influence of insulation thermal aging on the temperature assessment in electrical machines," *IEEE Trans. Energy Convers.*, vol. 36, no. 1, pp. 456–467, Mar. 2021, doi: 10.1109/TEC.2020.3001053.

[13] G. Biondi, "Corona resistant enamels developed in elantas europe: An opportunity for sustainability," in *Proc. IEEE 4th Int. Conf. Dielectrics (ICD)*, Jul. 2022, pp. 489–493, doi: 10.1109/ICD53806.2022.9863234.

[14] F. Guastavino, A. Ratto, E. Torello, L. D. Giovanna, G. Biondi, and G. Loggi, "Partial discharges measurements on conventional and nanocomposite enameled wires varying the ambient conditions," in *Proc. IEEE Int. Conf. Solid Dielectrics (ICSD)*, Jun. 2013, pp. 298–301, doi: 10.1109/ICSD.2013.6619755.

[15] W. Link. *Zeusinc.* Accessed: Oct. 31, 2022. https://www.zeusinc.com/wp-content/uploads/2020/05/PEEK-Insulated-Wire-V2R3.pdf

[16] *Standard Test Method for Thermal Endurance of Film-Insulated Round Magnet Wire*, document D2307 2007a, ASTM International, West Conshohocken, PA, USA, 2007.

[17] *Rotating Electrical Machines—Part 18–31: Functional Evaluation of Insulation Systems—Test Procedures for Form-Wound Windings—Thermal Evaluation and Classification of Insulation Systems Used in Rotating Machines*, document IEC 60034-18-31 Ed. 2.0, 2012, pp. 1–34.

[18] M. Farahani, E. Gockenbach, H. Borsi, K. Schäfer, and M. Kaufhold, "Behavior of machine insulation systems subjected to accelerated thermal aging test," *IEEE Trans. Dielectr. Electr. Insul.*, vol. 17, no. 5, pp. 1364–1372, Oct. 2010.

[19] H. Naderiallaf, P. Giangrande, and M. Galea, "A contribution to thermal ageing assessment of glass fibre insulated wire based on partial discharges activity," *IEEE Access*, vol. 10, pp. 41186–41200, 2022.

[20] J.-W. Jung and J.-S. Jung, "The effect of thermal ageing on the electrical characteristics of insulating oil for pole transformers," in *Proc. Int. Conf. Condition Monitor. Diagnosis*, Apr. 2008, pp. 303–306, doi: 10.1109/cmd.2008.4580287.

[21] J. Liu, Y. Xu, X. Wei, and X. Li, "Research of dielectric spectroscopy on insulation ageing assessment of XLPE cables," in *Proc. Annu. Rep. Conf. Electr. Insul. Dielectric Phenomena*, Oct. 2013, pp. 140–143, doi: 10.1109/CEIDP.2013.6747454.

[22] M. Ritamäki, "Effects of thermal aging on polymer thin film insulations for capacitor applications," M.S. thesis Fac. Comput. Elect. Eng., Tampere Univ. Technol., Tampere, Finland, 2014. [Online]. Available: https://trepo.tuni.fi/handle/123456789/22603?show=full

[23] V. Madonna, P. Giangrande, and M. Galea, "Evaluation of strand-to-strand capacitance and dissipation factor in thermally aged enamelled coils for low-voltage electrical machines," *IET Sci., Meas. Technol.*, vol. 13, no. 8, pp. 1170–1177, Oct. 2019.

[24] V. Madonna, P. Giangrande, and M. Galea, "Weibull distribution and geometrical size factor for evaluating the thermal life of electrical machines' insulation," in *Proc. IECON 46th Annu. Conf. IEEE Ind. Electron. Soc.*, Oct. 2020, pp. 1114–1119, doi: 10.1109/IECON43393.2020.9255227.

[25] T. W. Dakin, "Electrical insulation deterioration treated as a chemical rate phenomenon," *Trans. Amer. Inst. Electr. Eng.*, vol. 67, no. 1, pp. 113–122, Jan. 1948.

[26] A. Rumi, L. Lusuardi, A. Cavallini, M. Pastura, D. Barater, and S. Nuzzo, "Partial discharges in electrical machines for the more electrical aircraft. Part III: Preventing partial discharges," *IEEE Access*, vol. 9, pp. 30113–30123, 2021.

MUHAMMAD RAZA KHOWJA received the B.Eng. degree (Hons.) in electrical power engineering from the Mehran University of Engineering and Technology, Jamshoro, Pakistan, in 2011, the M.Sc. degree in electrical engineering, in 2012, and the Ph.D. degree in electrical and electronics engineering from the University of Nottingham, U.K., in 2018. He is currently a Research Fellow with the Power Electronics, Machines, and Control (PEMC) Group, University of Nottingham. His main research interests include integrated passive components, design and development of high-performance electrical machines for aerospace applications, and characterization of insulating materials for electrical machine's applications.

GAURANG VAKIL (Member, IEEE) received the Ph.D. degree in variable speed generator design for renewable energy applications from the Power Electronics, Machines, and Drives Group, Indian Institute of Technology Delhi, New Delhi, India, in 2016. Subsequently, he was a Research Associate with the Power Electronics, Machines, and Controls Group, University of Nottingham, Nottingham, U.K., where he was appointed as an Assistant Professor with the Electrical and Electronics Engineering Department, in 2016. His main research interests include design and development of high-performance electrical machines for transport and propulsion, optimizing electric drive-train for pure electric and hybrid vehicles (aerospace and automotive), high power density machines, and magnetic material characterization.

SYED SHAHJAHAN AHMAD received the B.E. degree in electrical engineering from the Indian Institute of Engineering Science and Technology, Shibpur, India, in 2012, and the M.E. and Ph.D. degrees in electrical engineering from the Indian Institute of Science Bangalore, Bengaluru, India, in 2014 and 2020, respectively. He is currently with the Power Electronics, Machines, and Control Group, University of Nottingham, U.K., as a Research Fellow. His research interests include design and control of electric machines, high-speed electric drives, power electronic converters, and modeling and control of power electronic systems. He was the recipient of Nampet-II Student Project Award for his master's work from the Department of Electronics and Information Technology, Government of India, in 2014.

RAMKUMAR RAMANATHAN received the B.Tech. degree in electrical engineering from Anna University, India, in 2014. He is currently pursuing the combined M.Tech. and Ph.D. degree with the Indian Institute of Technology Bombay, Mumbai, India. He is also a Research Associate with the University of Nottingham, U.K. His research interests include design of high-speed motors for electric vehicles and aerospace applications and modeling of advanced magnetic materials.

CHRIS GERADA (Member, IEEE) received the Ph.D. degree in numerical modeling of electrical machines from the University of Nottingham, Nottingham, U.K., in 2005. Subsequently, he was a Researcher with the University of Nottingham, on high-performance electrical drives and on the design and modeling of electromagnetic actuators for aerospace applications. Since 2006, he has been the Project Manager of the GE Aviation Strategic Partnership. He was appointed as a Lecturer (2008) of electrical machines, an Associate Professor (2011), and a Professor (2013) with the University of Nottingham. His main research interest includes the design and modeling of high-performance electric drives and machines. He is the past Chair of the IEEE IES Electrical Machines Committee. He is an Associate Editor of IEEE Transactions on Industry Applications.

MAAMAR BENAROUS received the Master of Science degree in electrical engineering from the University of Algiers and the Ph.D. degree in electrical engineering/machines and drives from the University of Bath, U.K., in 1997.

He has been with Collins Aerospace for over 24 years, where he currently holds the position of a Senior Technical Fellow. Prior to this role, he held various positions in both academia and industrial settings. He has written over 30 published technical papers in renowned journals and international conferences, such as IEEE and IET. He has also presented at international technical forums in Europe, Japan, and the USA. He holds 12 granted patents and nine published patents. His area of interest is in the field of high-power density electrical machines and drives and electromagnetic devices for aerospace applications, fault tolerant architecture, electrical motor reliability, and prognostic and diagnostic for electrical actuators.

• • •